The structure of porin from *Paracoccus denitrificans* at 3.1 Å resolution

A. Hirsch[a], J. Breed[a], K. Saxena[b], O-M.H. Richter[b], B. Ludwig[b], K. Diederichs[a], W. Welte[a],*

[a]*Universität Konstanz, Fakultät für Biologie, Universitätsstraße 10, 78464 Konstanz, Germany*
[b]*Institut für Biochemie, Molekulare Genetik, Universität Frankfurt, Marie-Curie-Straße 9, 60439 Frankfurt, Germany*

Abstract The crystal structure of a non-specific porin from *Paracoccus denitrificans* at 3.1 Å resolution has been solved by molecular replacement using the porin from *Rhodopseudomonas blastica* as the search model. *Paracoccus* porin is very similar to other non-specific porins of known structure: a trimer of 16 stranded β-barrels each with a central pore constricted by a long extracellular loop folding back against the barrel wall. The distinctive distribution of charged residues of this non-specific porin contributes to understanding the relation between structure and ion selectivity.

© 1997 Federation of European Biochemical Societies.

Key words: Porin; Membrane protein structure; X-Ray structure; Molecular replacement; *Paracoccus denitrificans*

1. Introduction

Porins are found in the outer membranes of Gram-negative bacteria, mitochondria and chloroplasts. They form weakly ion-selective channels for small hydrophilic molecules with size-exclusion limits around 600 Da [1,2]. Porins form stable homotrimers that are resistant to detergents and proteases. The structures of a number of porins are known with an anti-parallel β-barrel as the common core motif [3–6]. The barrel is comprised of 16 strands in non-specific and 18 strands in sugar-specific porins. The central pore along the axis of the barrel is constricted by long loops folding back into the barrel from the extracellular side. In the various theories of the origin of the eukaryotic cell [7], an endosymbiotic link between mitochondrial and *Paracoccus denitrificans* [8,9] is proposed. This is experimentally supported by electron microscopy of the voltage-dependent anion channel of mitochondrial outer membrane, indicating a structural relationship between mitochondria and bacterial porins [10]. The structure reported here may in the future contribute to the understanding of this evolutionary relationship.

2. Materials and methods

The purification and crystallisation of *Paracoccus* porin have been previously described [11]. Two crystal forms of space group P1 are found. The form used has cell dimensions $a = 92.2$ Å, $b = 100.7$ Å, $c = 111.8$ Å and $\alpha = 108.4°$, $\beta = 105.8°$, $\gamma = 108.6°$. Diffraction data were collected using a rotating anode source (STOE, Darmstadt, Germany) and a STOE imageplate detector system. A data set to 3.16 Å resolution of 71.4% completeness and $R_{sym} = 8.3\%$ was collected, containing 40 907 unique reflections. Data reduction and space group determination were carried out in XDS [12]. The asymmetric unit contains two trimers of *Paracoccus* porin. Non-crystallographic symmetry (NCS) relations were determined by a self-rotation function.

The results showed that the three-fold axes of each trimer lie anti-parallel to each other – trimer B packing head-to-head with trimer A and tail-to-tail with symmetry mates of A – and that trimer B is staggered with respect to trimer A by approx. 60° around their anti-parallel three-fold axes.

Rotation and translation functions were calculated using a trimer of *Rhodopseudomonas blastica* [4] porin (PDB code 1PRN) as the search model. Model structure factors were calculated in a triclinic cell of dimensions $a = b = 120$ Å, $c = 100$ Å and $\alpha = \beta = \gamma = 90°$ with a resolution range of 10–4 Å. Native and model structure factors were normalised prior to Patterson calculations. The rotation function was calculated in AMoRe [13] with a step size of 2.5° and a resolution range of 35–5 Å. Six maxima were obtained, corresponding to 120° rotations around the NCS axis for trimers A and B. One of the three possible orientations of trimer A was chosen at $K = 52.5°$, $\varphi = 89.8°$, $\phi = 147.6°$; that of trimer B was found by the previously determined NCS relation to trimer A. The orientation was improved by Patterson correlation refinement in X-PLOR [14], which increased the correlation coefficient to 0.344. Due to the low symmetry of the triclinic cell, the translation search reduces to finding the relative positions of the two trimers. Trimer A was centred on the origin of the triclinic cell and a three-dimensional translation search for trimer B was carried out on a 1 Å grid. A clear maximum was found at 0.075, 0.536, 0.666, giving a peak 11σ greater than the mean. The position of trimer B was further improved by rigid-body refinement.

Initial phases were determined and a first electron density map calculated. After six-fold non-crystallographic symmetry averaging and solvent flattening the mainchain was traceable in a $2F_o - F_c$ map. Initially, all B factors were set to 30. After 160 cycles of least-squares refinement, a slow cooling with start temperature of 4000 K was run. The resultant model gave an R factor of 37.5% ($R_{free} = 40\%$) and served as the start point for further refinement. Eight macrocycles of refinement were carried out, each comprising of manual adjustment of the model in O [15], rigid-body refinement, least-squares refinement, a slow cool refinement and grouped B-factor refinement. Strict non-crystallographic symmetry was applied initially and late in refinement replaced by strong NCS restraints of atomic positions and temperature factors. The starting temperature of the slow cool refinement was reduced from 4000 to 1000 K from the first to the eighth macrocycle. To avoid model bias the R_{free} [16] was carefully monitored, a decrease being observed at the completion of each cycle. The final model gives an R factor of 24.4% and R_{free} of 27.8%. The rms deviations from ideal bond lengths and bond angles are 0.007 Å and 1.24°, respectively. Due to the limited resolution of this study water molecules were not included in the model. However, one calcium ion per monomer was identified in difference Fourier maps based on its binding geometry.

3. Results

Paracoccus porin has the same fold as other non-specific porins, a 16 stranded anti-parallel β-barrel. The length of the strands ranges from 7 to 16 residues and their tilt from the membrane normal between 35 and 55°. The disposition of the strands is reflected in the height of the barrel wall, being 27 Å at the inner monomer-monomer contact surface and 33 Å at the membrane interface. Each trimer thus seems to form three independent pores through the membrane. The loops between strands are shorter at the periplasmic face (2–4 residues) than at the extracellular face (4–50 residues). The lon-
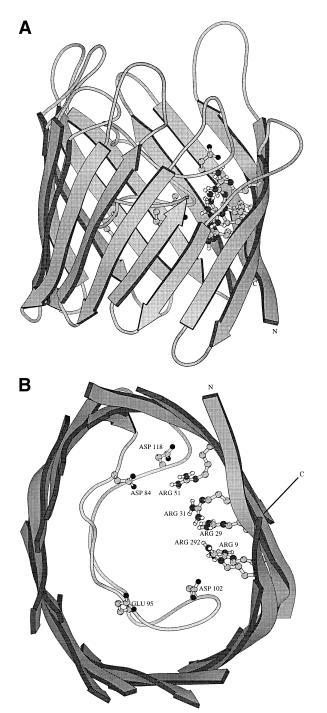
*Corresponding author. Fax: (49) (7531) 883183.

A

B

Fig. 1. (A) Ribbon representation of *Paracoccus* porin monomer. The shorter β-strands at the monomer-monomer interface are towards the observer. The extracellular face of the barrel is at the top; the difference in length between extracellular and periplasmic loops is evident. The termini are labelled and the charged residues of the pore constriction site are shown in ball-and-stick representation. (B) View along pore axis from the periplasmic face of *Paracoccus* porin monomer. The trimer axis lies outside of the barrel between the N- and C-termini. For clarity, only the barrel wall and loop 3 are shown. The pore constriction site is illustrated with the arginine cluster on the barrel wall and the negative charge cluster on loop 3 shown in ball-and-stick representation and labelled. The numbers of positive and negative charges are almost balanced (5 to 4), in contrast to cation-selective porins. The sidechains of the arginine cluster are closely packed, indicating a strong electrostatic field in this region.

gest extracellular loop (L3) is between strands 5 and 6 and, in common with other porins, folds back into the interior of the barrel and constricts the pore (Fig. 1).

The constriction site of the pore lies about halfway down the barrel; the pore is elliptical here with a free cross-section of approximate dimensions 13 Å×11 Å. There is a strongly asymmetric charge distribution at the pore constriction with a cluster of five basic residues (all arginine) at the barrel wall and four acidic on loop 3, giving rise to strong electrostatic fields transverse and parallel to the pore axis. Two girdles of aromatic residues run across the outer face of the barrel, with a vertical separation of 20–25 Å. Between these two girdles, the surface of the barrel is composed of hydrophobic residues, mostly alanine, valine and leucine. The aromatic girdles appear to mark the boundaries of the barrel surface interacting with the hydrophobic core of the membrane. This structural feature is found in certain other membrane proteins of known structure [3–6,17–20].

The functional unit of porins is the trimer; these are exceptionally stable, resistant to detergents and heat. Previous structures show significant contacts between the monomers [3–6] and this is also the case with *Paracoccus* porin. The solvent-accessible area of the monomer is 14 000 Å^2, that of the trimer is 34 090 Å^2. Each monomer-monomer contact area is thus 2636 Å^2. In total, 57 out of the 295 residues of each porin monomer are found at the trimer interface. Due to the arrangement of porin trimers with respect to each other in the asymmetric unit, the extracellular face of one trimer is opposed to that of the trimer above, the periplasmic face being opposed to that of the trimer below. The crystal contacts of *Paracoccus* porin are mostly hydrogen bonds between polar sidechains in these opposed sets of loops. There is also a contact involving a calcium ion bound by two Asp-189 residues in the extracellular loop between strains 9 and 10 of opposed trimers. This observation would explain the absolute necessity of rather high concentrations of calcium for the crystallisation of *Paracoccus* porin.

4. Discussion

In spite of the low completeness and resolution of our data, the structure of *Paracoccus* porin presented here is overall of good quality, mainly as it is the result of six-fold averaging. There are 17 outlier residues [21] in the Ramachandran plot, 11 of which lie very close to the core regions; the other six are in loops with weak electron density and may well adopt more favourable conformations in a higher resolution structure. We are seeking to improve the resolution of the data by a number of means, including mutating residues involved in crystal contacts. *Paracoccus* porin is very similar in structure to other non-specific porins, having the same features of overall fold, disposition of loop 3 and aromatic girdles. The pore size is similar to that of other non-specific porins as is the unit conductance in 1 M KCl-3.2 nS [22]. The main difference between *Paracoccus* and other non-specific porins is the distribution of charges at the pore constriction site. In most non-specific porins of known structure, negative charges dominate [3,4] and the porins are cation-selective [23,24]; except PhoE [5] where positive charges dominate and which is anion selective. In *Paracoccus* the number of positive and negative charges is almost balanced and *Paracoccus* porin is non-selective [22]. Thus, it seems that the balance of charges in the pore con-

striction site is the key to ionic selectivity in porins. This proposal is supported by the observed effects on ionic selectivity of porins upon the introduction of additional charges by chemical modification [23] or site-directed mutagenesis [25].

References

[1] Nikaido, H. and Vaara, M. (1985) Microbiol. Rev. 49, 1–32.

[2] Welte, W., Nestel, U., Wacker, T. and Diederichs, K. (1995) Kidney Int. 48, 930–940.

[3] Weiss, M.S., Kreusch, A., Schiltz, E., Nestel, U., Welte, W., Weckesser, J. and Schulz, G.E. (1991) FEBS Lett. 280, 379–382.

[4] Kreusch, A., Neubüser, A., Schiltz, E., Weckesser, J. and Schulz, G.E. (1994) Protein Sci. 3, 58–63.

[5] Cowan, S.W., Schirmer, T., Rummel, G., Steiert, M., Ghosh, R., Pauptit, R.A., Jansonius, J.N. and Rosenbusch, J.P. (1992) Nature 358, 727–733.

[6] Schirmer, T., Keller, T.A., Wang, Y.F. and Rosenbusch, J.P. (1995) Science 267, 512–514.

[7] Gupta, R.S. and Golding, G.B. (1996) Trends Biochem. Sci. 21, 166–171.

[8] John, P. and Whatley, F.R. (1975) Nature 254, 495–498.

[9] John, P. and Whatley, F.R. (1977) Adv. Bot. Res. 4, 51–115.

[10] Manella, C.A. (1992) Trends Biochem. Sci. 17, 315–320.

[11] Hirsch, A., Wacker, T., Weckesser, J., Diederichs, K. and Welte, W. (1995) Proteins 23, 282–284.

[12] Kabsch, W. (1988) J. Appl. Crystallogr. 21, 916–924.

[13] Navazza, J. (1994) Acta Crystallogr. A50, 157–163.

[14] Brünger, A.T. (1990) X-PLOR Manual, Yale University, New Haven, CO.

[15] Jones, T.A. and Kjeldgaard, M. (1990) Manual for O, Uppsala University, Uppsala, Sweden.

[16] Brünger, A.T. (1992) Nature 335, 472–474.

[17] Deisenhofer, J. and Michel, H. (1989) Science 245, 1463–1473.

[18] Henderson, R., Baldwin, J.M., Ceska, T.A., Zemlin, F., Beckmann, E. and Downing, K.H. (1990) J. Mol. Biol. 213, 899–929.

[19] Iwata, S., Ostermeier, C., Ludwig, B. and Michel, H. (1995) Nature 376, 660–669.

[20] McDermott, G., Prince, S.M., Freer, A.A., Hawthornthwaite-Lawless, A.M., Papiz, M.Z., Cogdell, R.J. and Isaacs, N.W. (1995) Nature 374, 517–521.

[21] Kleywegt, G.J. and Jones, T.A. (1996) Structure 4, 1395–1400.

[22] Wiese, A., Schröder, G., Brandenburg, K., Hirsch, A., Welte, W. and Seydel, U. (1994) Biochim. Biophys. Acta 1190, 231–242.

[23] Przybylski, M., Glocker, M., Nestel, U., Schnaible, V., Blüggel, M., Diederichs, K., Weckesser, J., Schad, M., Schmid, A., Welte, W. and Benz, R. (1996) Protein Sci. 5, 1477–1489.

[24] Butz, S., Benz, R., Wacker, T., Welte, W., Lustig, A., Plapp, R. and Weckesser, J. (1993) Arch. Microbiol. 14, 226–230.

[25] Bauer, K., Struyvé, M., Bosch, D., Benz, R. and Tommassen, J. (1989) J. Biol. Chem. 264, 16393–16398.